Aeroelastic Tailoring of Helicopter Main Rotor Blade

Francisco Campos Moreira Rodrigues
francisco.campos.moreira.rodrigues@tecnico.ulisboa.pt

Instituto Superior Técnico, Universidade de Lisboa, Portugal

October 2022

Abstract

The baseline concept of aeroelastic tailoring is to gain control over the in-flight deformation of a lifting surface to manipulate the generation of external aerodynamic loads, to improve the overall aircraft performance. Active and passive technologies have been significantly studied to evaluate the benefits of the aeroelastic methodologies. However, the implementation of passive aeroelastic tailoring methods in helicopter design is significantly understudied. In this thesis is intended to study the aeroelastic behavior of an elastic rotor blade model during flight. The study is framed to is evaluate if a single rotor blade can perform as a passive smart structure, adapting its geometry to different flight conditions, ultimately reducing the overall power consumption. A global evaluation integrating both aerodynamic and structural analyses is performed to predict the performance of the developed blade models in both hovering and forward flight conditions. A highly automated framework was designed to minimize the overall computational time and user input requirements, connecting all commercial software included in the project and automatically executing every major and intermediate procedure.
Keywords: Aeroelastic tailoring, aerodynamic analysis, structural analysis, automated framework

1. Introduction

Aeroelastic tailoring emerged as a design methodology in which the structural deformation of a lifting surface is directed to achieve aircraft performance objectives which are not conventionally related to structural design. The baseline concept of this methodology is to control in-flight deformation to manipulate the generation of external aerodynamic loads. Substantial research has been dedicated to aerodynamic tailoring in recent years [1]. Different technologies have been implemented to exploit the benefits, which can essentially be grouped in active and passive technologies, relying on materials and structural designs that can impact the stiffness, mass, or aerodynamics of an aircraft wing, requiring no external energy. Multiple methodologies of aeroelastic tailoring have been employed in helicopter design to improve the overall aircraft performance, particularly regarding active technologies. Nonetheless, the implementation of passive aeroelastic tailoring methods is significantly understudied, despite being based on a similar methodology as the active control technologies.

In this thesis, it is intended to study the aeroelastic behavior of an elastic rotor blade model during flight, particularly for hovering and forward flight regimes. This study is framed to evaluate if a single rotor blade can perform as a passive smart structure, adapting its geometry to different flight conditions with no control system, and ultimately reduce the overall power consumption.

2. Methodology

2.1. Rotor Analysis

The blade element momentum theory (BEMT) is often used to analyze rotor aerodynamics and global performance, as well as in rotor design. This is due to the simplicity of the methodology supporting the calculations, with reduced computational costs associated, enabling rapid analysis for different flight regimes. Despite the simplicity of the BEMT models, these produce efficient and accurate overall predictions [2, 3, 4].

BEMT comprises the main principle of the blade element theory, dividing the rotor blade in several blade elements with no mutual influence of adjacent sections. Since this theory assumes blade sections as two-dimensional airfoil profiles that generate aerodynamic forces and moment, the predictions of rotor performance based in this theory directly depend on the airfoil performance.

Airfoil Performance

For a prescribed pitch distribution along the blade span, it is required to compute the local velocity for each blade section to estimate the angle of attack. By computing the local fluid velocity, and subsequently calculating the local Reynolds and Mach, all parameters required to evaluate the

airfoil performance are determined.

Blade Performance

The rotor blade performance is evaluated based on the nondimensional coefficients retrieved from the performance analysis of each blade section. The total lift and drag generated by the rotor blade can be computed by integrating the incremental lift and drag along the blade span, which can be simplified to a some of the contributions of each blade element.

2.2. Structural Analysis

A structural analysis allows to determine the influence of the external aerodynamic loads by predicting important parameters such as stress, strain, displacement, and rotations. These results can ultimately dictate whether the studied model is adequate to the project or not.

Load Cases

The distributed pressure to which the rotor blade is subjected during flight can be predicted based on the chordwise pressure distribution acquired from the airfoil performance analysis of each blade section, converting the nondimensional pressure coefficient into local pressure applied on the surface, given the relation

$$p(x) = \frac{1}{2} C_p(x) \rho U^2 + p_\infty \tag{1}$$

in which C_p is the nondimensional pressure coefficient, ρ the fluid density, U the local fluid velocity and p_∞ the freestream static pressure.

In addition to the distributed pressure, the rotor blade is also subjected to centrifugal force. In a finite element analysis, the centrifugal force is formulated as a function of the finite element nodal coordinates and the angular velocity [5].

Boundary Counditions

The boundary conditions to be defined in the structural analysis are defined considering that the blade models are designed to be assembled in a bearingless rotor [6]. The studies on rotor blades performed for overall deformation and cross-sectional analyses are typically modeled based on moderate deflection-type beam theories. Each component can be discretized in beam elements, and the structural model based on intrinsic formulation of beams in a moving frame [7, 8, 9]. It is assumed that the flexbeam has sufficient stiffness to be approximated to a rigid body. In the finite element analysis, this assumption is equivalent to extending the boundary conditions imposed at the hub connection to the end of the root cut-out, restraining all degrees of freedom of every component, except the rotor blade.

Solver

The rotor blade's structural behavior is evaluated by performing a static stress analysis. This means the inertia effects are neglected, as well as any time-dependent effects. Since large displacements are expected, which represents a geometric nonlinearity, it is used a nonlinear analysis as the solving strategy. The loads are divided in smaller increments which are successively applied, allowing to assess the structure's behavior and to take into consideration the nonlinearities during the analysis.

2.3. Integration

The blade design, rotor and structural analyses are integrated in a multidisciplinary evaluation to predict the performance of the designed blade models during flight. The elastic rotor blade models are designed with a blade twist to present improved performance in terms of reducing power consumption, during forward flight condition. This model corresponds to the deformed geometry of the rotor blade after reaching static equilibrium. The global analysis is further performed to iteratively achieve the manufacturing geometry. Afterwards, the performance of the manufacturing blade model is evaluated for hovering flight conditions.

Forward Flight

In straight-and-level forward flight, all forces acting on the helicopter must be balanced: lift equals weight and drag equals thrust [10]. The magnitude of the horizontal thrust component is settled by the cyclic control, which allows to increase or decrease the airspeed, by defining the tilting level of the rotor disk plane. The magnitude of the lift component is corrected by the collective control, which allows to maintain the flying altitude [11]. Therefore, prior to initiating the global analysis, the aerodynamic analysis is iteratively performed with an adjustment of the cyclic and collective control inputs, to determine the configuration for which the required force equilibrium is achieved. This procedure is described in the flowchart presented in Figure 1.

The manufacturing geometry can be determined by unloading the aerodynamic loads to which the rotor blade is subjected. The unloading is simulated in the structural analysis by defining both load cases with a symmetrical magnitude.

Finishing the structural analysis, it is only possible to consider that the deformed geometry is a converged solution of the global analysis if the computed values of the deflection angle due to torsion, θ_T, is negligible. If not, the blade model must be updated to the deformed geometry, and the aerodynamic and structural analyses are repeated. This approach is commonly referred as *Two-Way Aeroelastic Coupling* [12]. The integration of the Two-Way Aeroelastic Coupling is illustrated in the flowchart presented in Figure 2.

Hovering Flight

In hovering flight, For an ideal no-wind condi-

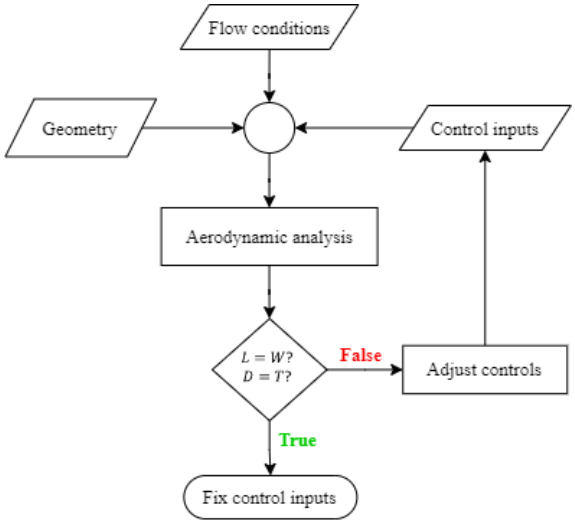

Figure 1: Iterative procedure to determine the control configuration providing the required force equilibrium for forward flight.

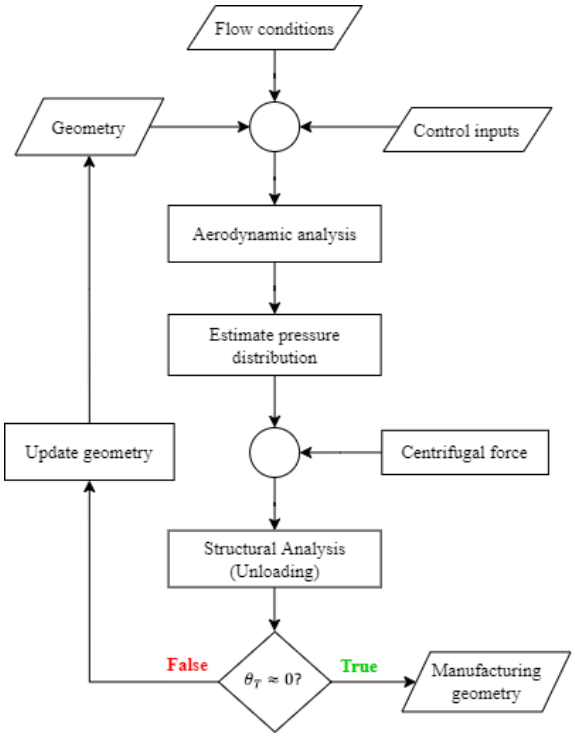

Figure 2: Integration of the *Two-Way Aeroelastic Coupling* in the analysis performed for forward flight.

tion, all opposing forces acting on the helicopter must be in balance, equaling the respective opposite [10]. Thus, lift equals weight, leading to a stationary hover. The generated lift can be adjusted to maintain the stationary state by moving the collective, which actively changes the pitch angle of all rotor blades [11]. As in forward flight conditions, the control configuration must also be adjusted in hovering flight, until the force equilibrium condition is satisfied.

The structural analysis is conducted based on the load prediction provided from the aerodynamic analysis, and the aeroelastic behavior of the rotor blade is evaluated based on the results. Following the considerations provided for the analysis in forward flight, the *Two-Way Aeroelastic Coupling* must be included in the hovering flight analysis as well. Concluding the global analysis, the results of the global analysis are compared with the performance of a rigid rotor blade for hovering flight conditions. Figure 3 presents the flowchart depicting the entire hovering flight analysis,

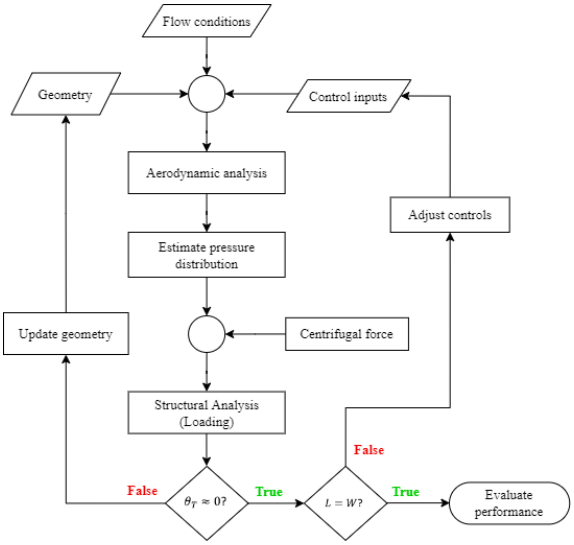

Figure 3: Integration of the *Two-Way Aeroelastic Coupling* in the analysis performed for forward flight.

3. Implementation

A highly automated framework was designed to minimize the overall computational time involved in the global analysis, by greatly reducing the need for user-interactivity. The framework was developed in *Python*, including several codes to automatically execute the aerodynamic and structural analyses of a given blade model, as well as every intermediate and final post-processing procedures involved in the global analysis. The aerodynamic analysis is performed in *XFOIL* and the structural analysis in *Abaqus FEA*, specifically in the *Abaqus/CAE*

environment. The developed blade models were designed in *Autodesk Fusion 360*.

3.1. Validation

The rotor blade models developed in this project were based on the main rotor of a *Sikorsky UH-60A Black Hawk*. The design characteristics and operational conditions regarding this rotor implemented in this project, are presented in Tabel 1. The mass of the helicopter was set as 8322.4 kg, based on the estimates provided by D. Han, V. Pastrikakis, and G. N. Barakos [13].

Table 1: *UH-60A* main rotor characteristics [14]

Rotor Parameters	
Blade chord length	0.5273 m
Number of blades	4
Rotor radius	8.1778 m
Nominal speed	27 rad/s

3.2. *XFOIL*

XFOIL is an interactive program for designing and analyzing isolated airfoils, particularly in subsonic environment, developed by M. Drela in 1986 [15]. The *XFOIL* design and analysis system is composed by a set of menu-driven algorithms to conduct a high-order, two-dimensional panel method and a viscous/inviscid coupling interaction method to predict drag, boundary layer transition and separation [16], as well as mixed-inverse and full-inverse design methods [17].

3.3. *Abaqus/CAE*

The implementation of *Abaqus/CAE* relies on a *Python* extension named *Abaqus Scripting Interface* [18]. Using the *Abaqus Scripting Interface*, the user can bypass the manual procedure and directly communicate with the kernel, submitting a *Python* with the intended commands.

Part Module

The structural components of the blade models are categorized in two major groups: the external structure, composed by the upper and lower parts of the blade skin, and the internal structure, which includes every structural component contained inside the blade skin. The partitioning process is focused on the external structure, since the aerodynamic loads and boundary conditions must be applied on the structural components exposed to the surrounding environment.

The blade skin is partitioned using a datum plane coincident with the origin xz-plane, to enhance the separation between the root cut-out and the rotor blade. The blade is consequently divided into two cells: the root cut-out, where boundary conditions are prescribed, and the rotor blade, where the aerodynamic loads are applied. For the upper and lower parts of the blade skin, a surface set containing the external face is created. The external faces of the root cut-out are directly saved to geometric sets., The upper and lower parts of the rotor blade are iteratively partitioned to divide the blade into the required number of blade elements.

Step Module

The finite element analysis to be performed in this project is a static stress/displacement analysis. Since it is expected a geometrically nonlinear behavior of the rotor blade, the large-displacement formulation is used. The initial increment was defined as 0.01 of the applied load, and the minimum increment size set to 10^{-6}. The size of the remaining increments is automatically selected by *Abaqus/CAE* based on an evaluation of the computational efficiency.

Property Module

For each material to be used in an analysis, it is required to specify a set of material behaviors and provide property data for each material behavior included. Only the properties necessary to define a material to be evaluated in a geometrically nonlinear static analysis were specified, such as density, Young's Modulus and Poisson's ratio.

Load Module

Part instances associated to each imported part must be created. All part instances are defined as dependent, corresponding to a pointer to the geometry of the original part. Any operation performed on the part, for example partitions, virtual topology, or mesh generation, is reflected on the part instance. In practical terms, a dependent part instance shares the geometry and mesh of the original part.

Mesh Module

For three-dimensional parts with complex geometries, the use of partitions to divide the part into simpler regions is an efficient strategy to gain more control over mesh generation. The resulting mesh of a partitioned part presents a grid of elements aligned with the partition, which means the mesh "flows" along the partition. The partitions performed in the upper and lower parts of the rotor blade ensure that each resulting edge comprises the necessary mesh nodes to further define the airfoil profile of each blade section to be evaluated in the aerodynamic analysis.

The finite element meshes of all parts of the studied were generated using tetrahedral elements, particularly second-order (quadratic) elements, which are labeled as $C3D10^{(S)}$ (10-node quadratic tetrahedron). These elements are defined by a non-linear shape function, providing results with higher accuracy than first-order (linear) elements for problems without impact, elaborate contact conditions

or substantial element distortion. In addition, these elements are more suitable for modeling complex geometric features, such as curved surfaces.

Interaction Module

The physical proximity of two regions associated with distinguished part instances is not sufficient to automatically imply any type of interaction between these part instances. A tie constraint allows to combine two distinguished regions even if the generated meshes are dissimilar. The DOF are constrained to prescribe relative motion between both regions. To create a tie constraint, it is necessary to identify the "master" and "slave" surfaces, containing the regions on which the constraint must be applied.

Load Module

The distributed pressure to which the rotor blade is subjected during flight is simulated by defining a surface-based pressure load, and prescribing to the surfaces of the upper and lower parts of the blade skin. The distribution field is defined using a mapped field, importing discrete parameter data from a XYZ point cloud data file, mapping the imported coordinates to locations in the model and applying the correspondent field value. The field value is equal to the local pressure estimated in the aerodynamic analysis. The centrifugal force is applied on the model by generating a rotational body force, and The type of boundary condition selected to prescribed to the root cut-out is defined as "ENCASTRE", in which all degrees of freedom are equal to zero.

Job Module

In addition to being able to run a full analysis in *Abaqus/CAE*, it is possible to restart a finite element analysis from an intermediate point and change the remaining load history data. To restart an analysis, it is necessary to request *Abaqus/CAE* to write the model definition and state on the required files to restart the analysis. To run a restart analysis of a job linked with a model, it is necessary to create a new model by copying the original one. The settings to reuse state data from a previous analysis are specified by editing the new model's attributes and redefine it to a restart model. It is required to identify the job from which the data is read, as well as the analysis step containing the desired restart location. Figure 4 shows the flowchart describing procedures to be followed for an exemplar restart analysis.

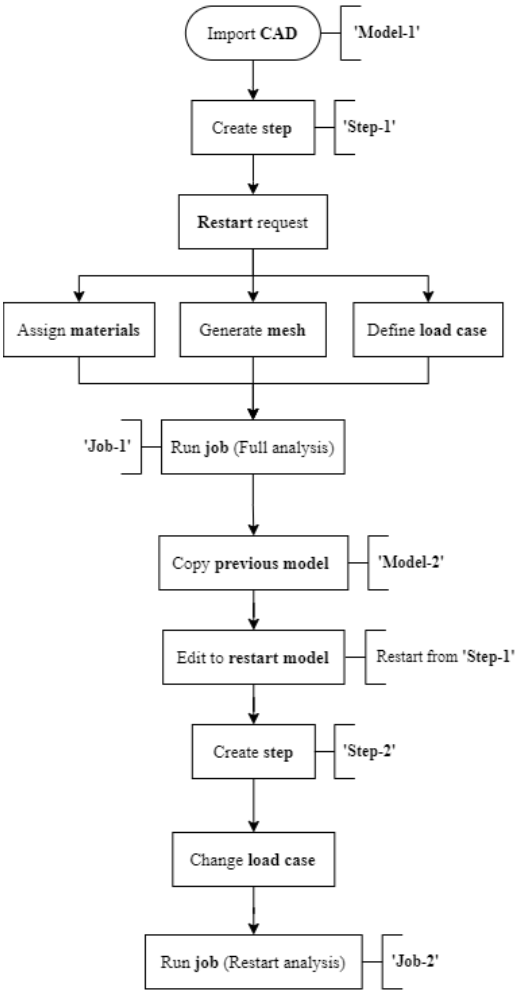

Figure 4: Procedures to be followed for an exemplar restart analysis.

3.4. Automated Framework

Initiate Model

The initial routine of the automated framework is for starting the *Abaqus/CAE* model. the step file (extension *.step*) is uploaded by creating an ACIS object containing a list of n *ACIS* bodies, where n is the number of bodies defined in the CAD model. The code was developed for the first (n-2) bodies to be assumed as internal structure components, and bodies (n-1) and n as the upper and lower components of the blade skin, respectively. Once all parts are imported, the partitioning procedure is performed. At last, the analysis step is created, followed by the field output and restart requests.

Afterwards, the blade is partitioned into the respective number of blade elements and the finite element mesh is generated. The coordinates of the nodes contained in each blade section are exported to specific text files, labeled with a name and number to identify the edge position and the part of the blade skin to which they are correspondent.

Forward Flight

The node coordinates are imported from both text files and rearranged into the correct order to generate the coordinate distribution file for *XFOIL*. The airfoil profile of each blade section presents an implicit pitch angle resulting from the blade twist

distribution. Therefore, a coordinate transformation is performed. The origin of the local coordinate system is positioned on the leading edge, the x-axis contains the profile's chord line, and the spanwise position of each blade section is given by the y-coordinate. The coordinate transformation is defined by a translation, followed by a rotation along the y-axis. The angle of rotation is equal to the blade twist at each section. The twist angle is quantified by estimating the chord line's inclination angle, given by the straight line containing the leading and trailing edges nodes. The local coordinates of the upper and lower surface are assembled in a single coordinate file and further submitted into *XFOIL*.

For each blade section, after automatically performing the two-dimensional aerodynamic analysis in *XFOIL*, the acquired chordwise pressure distribution is converted to local pressure distribution, and the estimated distribution is appended to a XYZ-format text file to define the pressure load in *Abaqus/CAE*. Afterwards, the centrifugal force is prescribed to all part instances and the analysis job is submitted.

The geometry of the deformed model is assessed by post-processing the structural analysis results, which are exported to the output database file. The output data to be used is contained in the field variable "COORDS", which holds the current nodal coordinates. The original point-cloud data files are updated with the nodal coordinates of the deformed model.

The *Two-Way Aeroelastic Coupling* is introduced in the framework after completing the primary analysis. The airfoil recognition procedure is repeated for the deformed geometry to update the pitch angles for each blade section. The difference in pitch angle is computed to evaluate the aeroelastic convergence. If the maximum obtained value is not negligible, the aerodynamic and structural analyses, as well as all intermediate operations, are repeated for the deformed geometry. The difference between the initial Abaqus/CAE model and the restart model resides in the load case defining the distributed pressure, since the aerodynamic loads are redistributed due to the elastic deformation of the rotor blade. Therefore, after copying the initial model, it is only necessary to create a new analysis step, in which it is created the load case defining the updated pressure distribution. Afterwards, the "Restart" job is submitted for analysis.

Hovering Flight

After reaching convergence in the analysis performed in forward flight, the manufacturing geometry is obtained, and its performance can be evaluated for hovering flight conditions. The entire analysis described in the previous section is used to study the manufacturing geometry. Nonetheless, the minor differences between the methodologies for hovering and forward flight, implied the adjustment particular input data and procedures within the analysis. First, the advance ratio is set to zero, to simulate a flight regime with null forward speed. The calculation of the local pressure distribution for each blade section is also modified, since for hovering flight, the blade model is effectively loaded with the real aerodynamic forces to which it is subjected during flight. Furthermore, since the analysis in hovering flight is initiated from a deformed geometry obtained from the forward flight analysis, the restart routine must be used for all iterations required. At last, it is required to include the iterative process of adjusting the collective control until achieving the vertical force equilibrium, where lift is equal to the helicopter's weight. After attaining aeroelastic convergence, the total lift is estimated. If the equilibrium condition is not satisfied, the input control is incremented, and the aerodynamic and structural analysis are repeated. If the equality is satisfied, the power consumption is estimated, and the global analysis is concluded.

4. Results

4.1. Blade Twist Characterization

The global analysis is conducted on a blade model designed with a blade twist for improved performance in reducing the power consumption for forward flight regime, equivalent to the deformed geometry after reaching static equilibrium during forward flight. Marco Lonoce [19] studied the influence of the blade twist distribution in rotor power consumption. Within the range of concepts tested, the quadratic distribution, given by

$$\theta(x) = ar^2 + br + c \tag{2}$$

revealed the minimum power consumption. The optimal solution was found for a = 11.43 and b = -22.86. Coefficient c is equivalent to the sum of all control inputs. The aerodynamic analysis for forward flight regime was iteratively performed to predict the control configuration for which the vertical force equilibrium is achieved. For the 4-bladed main rotor, the azimuth positions of each blade were fixed at 0°, 90°, 180° and 270°. The equilibrium was attained for a control configuration given by a collective input of 16.39° and a longitudinal cyclic input of -0.62°, for which the total lift generated is equal to approximately 81405 N, with a relative error of 0.29% comparing to the helicopter's weight. Thus, the pitch distribution can be written as

$$\theta(x, \psi) = 11.43r^2 - 22.86r + 16.39 - 0.61\psi \tag{3}$$

The same procedure was followed to estimate the control configuration for hovering flight conditions,

since it is used not only as an initial guess for the hovering flight cycle of the global analysis, but also for the performance evaluation after completing the global analysis, to compare the power consumption of the rigid and elastic model. The force equilibrium was achieved for a collective input of 19.4833°. Note that for hovering flight, the cyclic input is null.

4.2. Open Blade Profile

The blade concept proposed by Diogo Nascimento [20] served as a baseline for the developed blade models, and therefore its performance was evaluated in the global analysis. The model is composed by a Polyamide (Nylon, Type 46, Extrusion) blade skin with a gap in the lower part, at the trailing edge, resulting in an open profile. The gap was set to be 1.5 mm, enough to reduce the profile's stiffness, when compared to a closed file, with with negligible greater impact on the blade aerodynamics. The blade skin is dimensioned with 2.5 mm thickness and incorporates a spanwise reinforcement connecting the upper and lower parts, with equal thickness. It was positioned at approximately 46.22% equivalent to $x = 0.2437$ m.

The results of the structural analysis revealed a substantial deformation of the blade profile along the entire span, particularly at the blade tip. The airfoil shape is severely modified, to a stand of compromising the minimum performance requirements. Furthermore, the deformed model presented a significantly large deflection due to bending. This deflection is quantified as the mean value of displacement in the z-coordinate between the leading and trailing edge. It was estimated a value of approximately 0.2851 m. The outcome of the analysis conducted on the open profile blade forced the rejection of the proposed concept

4.3. Closed Blade Profile

It was introduced the concept of closing the titanium blade skin with a material with a reduced Young's Modulus, to improve the torsional stiffness of a conventionally closed profile. The final model is composed by a 7.5 mm thickness titanium blade skin, with a Polyamide strip of equal thickness, connecting the upper and lower parts of the blade skin. Multiple 7.5 mm thickness stringers were incorporated in blade skin along the blade chord, with equal spacing between each stringer. At 25% of the blade chord, the stringers are arranged in a "X" scheme with 1.41 m of length, approximately 25% of the blade length, which is repeated until reaching the blade tip.

Forward Flight

Regarding the forward flight cycle included in the global analysis, nine iterations were required to achieve aeroelastic convergence. The maximum value of deflection is obtained within the first iteration, with a reduction of 2.90° of pitch angle at the blade tip. From the second iteration forward, the elastic deformation is partially recovered, with the pitch angle at the blade tip being increased until reaching aeroelastic convergence. It was estimated a total decrease of the pitch angle at the blade tip of 1.01°, which is a reduction of 34.88% in face of the value determined for the first iteration. The difference between the blade root and tip pitch angles was increased from 5.44° to 6.45°, leading to a blade tip with greater twist.

Hovering Flight

After determining the manufacturing geometry, the hovering flight iterative cycle was conducted to evaluate the blade performance within this flight regime. For the initial guess of the collective input, it was used the same value obtained for the rigid blade to satisfy the vertical force equilibrium condition.

Within the first cycle, the first iteration revealed significant torsional deflection along the blade span, with an estimated increase in pitch angle of 4.45° at the blade tip. The torsional deflection is increased from the second iteration forward, until reaching aeroelastic convergence. Finishing the first cycle, it was estimated a total increase in pitch angle at the blade tip of 5.10°, which is a rise of 14.73% comparing to the value obtained for the first iteration. For the resulting blade geometry, it was determined a total lift of 37062.13 N generated by the rotor blade, significantly surpassing the required lift to attain the vertical force equilibrium.

Prior to the second cycle, the collective input was decreased in 3.5°. The results revealed a stable aeroelastic behavior, with convergence being achieved after few iterations. The results revealed a total decrease of pitch angle at the blade tip of 0.0651°. The error margin relative to the required lift was reduced to 24.35%, being estimated a total lift generation of 25381.06 N.

The third cycle was performed after reducing the collective input by 1°. Slight variations in the pitch angle were registered between both iterations, leading to a total decrease of 0.02°. It was estimated a total lift generation of 20628.03, reducing the relative error to 1.06%, which was considered reasonable value to assume that the vertical force equilibrium condition is satisfied. Comparing with the manufacturing geometry, the difference in pitch angle between the blade root and tip is significantly reduced, decreasing from 6.45° to 1.44°, ultimately leading to a low twisted blade.

Rotor Power Consumption

Since it is assumed a uniform inflow distribution along the blade, the induced power coefficient, is equal for the rigid and elastic model blade. There-

fore, the difference in power consumption between both models directly depends on the rotor profile power coefficient. Given a rotor solidity of 0.0821, the results show that the elastic blade reduced the rotor profile power coefficient by a minimal margin of 0.5%. This result is supported by the increased angles of attack in the rigid blade model for more than half the blade span (approximately 58%), contributing to higher values the nondimensional drag coefficient.

5. Conclusions

Several blade models were evaluated along the concept development process, despite only a few being addressed in this document. The different models studied can be categorized in two main concepts: open profile blades and closed profile blades. The open profile blades were designed based on the concept proposed by Diogo Nascimento [17]. This concept was tested in the global analysis and revealed substantial deformation along the blade span. The blade profile was excessively altered during flight conditions, with significant values of deflection due to bending registered as well, leading to a rejection of the concept.

It was further introduced the concept of closing the profile with a material presenting significant lower Young's modulus when compared to the blade skin. This concept was sequentially refined, and the final model was submitted to the global analysis. From the forward cycle, it was obtained a manufacturing geometry with greater blade twist comparing with the forward flight geometry, with the difference between the pitch angles at the blade root and tip increasing from 5.44° to 6.45°. After conducting the analysis for hovering flight conditions, the torsional deflection along the blade span substantially increased the blade twist, with the difference of pitch angle being reduced from 6.45° to 1.44°, resulting in a considerably low twisted blade, close to a linear pitch distribution. Despite the performance results revealing a minimal reduction of the power consumption, the final geometry does not allow to validate the proposed concept. The main objective of the adaptive blade concept is to increase the blade twist in hovering flight and increase for forward flight, which was not achieved with the final blade model. The reduction in power consumption is only observed due to the inform flow assumption for both rigid and elastic blade models, which lead to equal induced power coefficients. The impact of the blade twist on the inflow distribution is not considered, justifying the unnoticeable impact of a less twisted blade in the power consumption estimates for hovering flight.

References

[1] C. Jutte and B. Stanford. Aeroelastic tailoring of transport aircraft wings: State-of-the-art and potential enabling technologies. Technical report, National Aeronautics and Space Administration (NASA), 2014.

[2] N. A. R. Abdullah N. A. R. Nik Mohd M. F. Yaakub, A. A. Wahab and S. S. Shamsuddin. Aerodynamic prediciton of helicopter rotor in forward flight using blade element theory. *Journal of Mechanical Engineering and Sciences*, 2017.

[3] N. D. Mittal N. Tenguria and S. Ahmed. Investigation of blade performance of horizontal axis wind turbine based on blade element momentum theory (bemt) using naca airfoils. *International Journal of Engineering, Science and Technology*, 2010.

[4] Joseph Carroll and David Marcum. Comparison of a blade element momentum model to 3d cfd simulations for small scale propellers. *SAE Int. J. Aerosp.*, 2013.

[5] Joseph Carroll and David Marcum. Effect of the centrifugal forces on the finite element eigenvalue solution of a rotating blade: A comparative study. *Multibody System Dynamics*, 2008.

[6] Dewey H. Hodges. Aeromechanical stability analysis for bearingless rotor helicopters. *Journal of American Helicopter Society*, 1979.

[7] H. C. Seong S. J. Shin Y. J. Kee T. Y. Chun, H. Ryu and D. K. Kim. Structural analysis of a bearingless rotor using an improved flexible multibody model. *Journal of Aircraft*, 2013.

[8] In Lee In-Gyu Lim. Aeroelastic analysis of bearingless rotors with a composite flexbeam. *Composite Structures*, 2009.

[9] Dewey H. Hodges. A mixed variational formulation based on exact intrinsic equations for dynamics of moving beams. *International Journal of Solids and Structures*, 1990.

[10] Federal Aviation Administration (FAA). Aerodynamic of flights. In *Helicopter Flying Handbook*, chapter 2, page 29. Aviation Supplies Academics (ASA), 2019.

[11] Federal Aviation Administration (FAA). Basic flight maneuvers. In *Helicopter Flying Handbook*, chapter 9, page 20. Aviation Supplies Academics (ASA), 2019.

[12] D. P. Brandão. Development of a framework for static aeroelastic analysis of flexible wings including viscous flow effects. Master's thesis, Instituto Superior Técnico, 2015.

[13] V. Pastrikakis D. Han and G. N. Barakos. Helicopter performance improvement by variable rotor speed and variable blade twist. *Aerospace Science and Technology*, 2016.

[14] Joseph Totah. A critical assessment of uh-60 main rotor blade airfoil data. Technical report, National Aeronautics and Space Administration (NASA), 1993.

[15] *XFOIL: An Analysis and Design System for Low Reynolds Number Airfoils*, 1989.

[16] Mark Drela and Michael B. Giles. Viscous-inviscid analysis of transonic and low reynolds number airfoils. *AIAA Journal*, 1987.

[17] E. Soinne and S. Laine. An inverse boundary element method for single component airfoil design. *Journal of Aircraft*, 1985.

[18] Simulia - Dassault Systèmes. *Abaqus Scripting User's Guide*.

[19] Marco Lonoce. Helicopter blade twist optimization in forward flight aerospace engineering. Master's thesis, Instituto Superior Técnico, 2016.

[20] Diogo Nascimento. Passive smart structure design for an adaptive helicopter blade. Master's thesis, Instituto Superior Técnico, 2018.